A Human Skin Model for Assessing Arboviral Infections

Allen T. Esterly[1], Megan G. Lloyd[1], Prashant Upadhyaya[2], Jennifer F. Moffat[1] and Saravanan Thangamani[1,3,4]

Arboviruses such as flaviviruses and alphaviruses cause a significant human healthcare burden on a global scale. Transmission of these viruses occurs during human blood feeding at the mosquito-skin interface. Not only do pathogen immune evasion strategies influence the initial infection and replication of pathogens delivered, but arthropod salivary factors also influence transmission foci. In vitro cell cultures do not provide an adequate environment to study complex interactions between viral, mosquito, and host factors. To address this need for a whole tissue system, we describe a proof of concept model for arbovirus infection using adult human skin ex vivo with Zika virus (flavivirus) and Mayaro virus (alphavirus). Replication of these viruses in human skin was observed up to 4 days after infection. Egressed viruses could be detected in the culture media as well. Antiviral and proinflammatory genes, including chemoattractant chemokines, were expressed in infected tissue. Immunohistochemical analysis showed the presence of virus in the skin tissue 4 days after infection. This model will be useful to further investigate: (i) the immediate molecular mechanisms of arbovirus infection in human skin, and (ii) the influence of arthropod salivary molecules during initial infection of arboviruses in a more physiologically relevant system.

JID Innovations (2022);**2:**100128 doi:10.1016/j.xjidi.2022.100128

INTRODUCTION

Arboviruses inflict a substantial global health burden on the human population. The re-emergence of Zika virus (ZIKV) in 2014–2015 in Brazil is evidence that previously identified pathogens can re-emerge to become significant health burdens on susceptible populations (Weaver et al., 2016). Other arboviruses, such as Usutu virus, Spondweni virus, and Mayaro virus (MAYV), continue to emerge (Pierson and Diamond, 2020). MAYV is a New World arthritogenic alphavirus with current autochthonous cycles of transmission in Central and South America (Diagne et al., 2020). Research on emerging arboviruses is needed to better understand transmission cycles that threaten human health.

Mosquitoes inject saliva made up of a complex mixture containing pathogens, bioactive proteins, and small RNAs to facilitate blood-feeding and pathogen transmission (Arcà and Ribeiro, 2018; Maharaj et al., 2015). These bioactive molecules regulate hemostasis and modulate mammalian immune responses at the mosquito-host-pathogen interface (Huang et al., 2019; Pingen et al., 2017). The transmission interface has been investigated using in vitro tissue culture or animal infection models, but these systems do not fully represent the human skin tissue environment. Therefore, this study intends to model arbovirus infection in human skin ex vivo to investigate the immediate immunological events during transmission.

Because the majority of mosquito-borne arboviruses transmitted to humans are from the genus Flavivirus or Alphavirus, we used an established flavivirus of medical relevance ZIKV and an emerging alphavirus MAYV. MAYV and ZIKV infect human skin and replicate up to 4 days after infection, shedding from the skin to culture media. Chemoattractant chemokines, along with proinflammatory and antiviral genes, were expressed in both MAYV and ZIKV infected skin as expected. In addition, immunohistochemical analysis revealed staining positive for the virus in skin 4 days after infection in both virus-infected groups. This model will be further used to determine how mosquito salivary factors influence viral replication kinetics or proinflammatory and chemoattractant molecule expression during infection.

RESULTS AND DISCUSSION

Viability of human skin explant

This study used human skin donated from elective breast reduction surgeries and cultured it ex vivo as previously described (Lloyd et al., 2020). Human skin was viable when cultured ex vivo for at least 4 days. Tissue sections stained with H&E showed minor histopathological changes after 4 days in culture. In addition, some papillary dermal edema and minimal lymphocytic infiltrate in the superficial dermis were observed; however, no major pathological changes, such as acanthosis or psoriasiform hyperplasia, were apparent (Figure 1).

[1]*Department of Microbiology and Immunology, SUNY Upstate Medical University, Syracuse, New York, USA;* [2]*Department of Surgery, SUNY Upstate Medical University, Syracuse, New York, USA;* [3]*SUNY Center for Vector-Borne Diseases, SUNY Upstate Medical University, Syracuse, New York, USA; and* [4]*Institute for Global Health and Translational Medicine, SUNY Upstate Medical University, Syracuse, New York, USA*

Correspondence: Saravanan Thangamani, Department of Microbiology and Immunology, SUNY Upstate Medical University, 505 Irving Avenue, Syracuse, New York 13210, USA. E-mail: thangams@upstate.edu

Abbreviations: IFITM, IFN-induced transmembrane protein; KC, keratinocyte; MAYV, Mayaro virus; ZIKV, Zika virus

Received 2 November 2021; revised 22 February 2022; accepted 9 March 2022; accepted manuscript published online XXX; corrected proof published online XXX

Cite this article as: JID Innovations 2022;2:100128

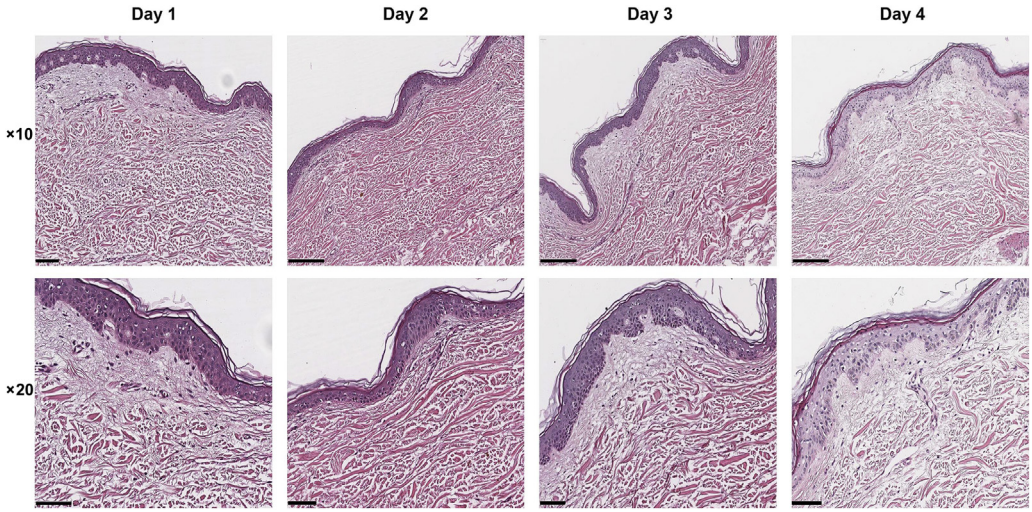

Figure 1. Viability of human skin ex vivo. Skin cultured ex vivo was harvested each day for up to 4 days. Formalin-fixed, paraffin-embedded tissue sections (5 μm) were placed on glass slides for H&E staining. Pathological interpretation was provided by a board-certified pathologist (HistoWiz, Brooklyn, NY). Sections are representative of multiple biological samples from multiple skin specimens sectioned and stained using the same methodology. Bar = 500 μm (×10 image) and 200 μm (×20 image).

MAYV and ZIKV replication in human skin

To determine the susceptibility of human skin to arbovirus infection, skin pieces were intradermally inoculated with 1,000 focus forming units of MAYV or ZIK23V, a physiologically relevant dose delivered from a mosquito (Castanha et al., 2020; Styer et al., 2007). Viral RNA in the skin tissue was measured by qRT-PCR and was increased for both MAYV and ZIKV during the 4-day incubation period (Figure 2). We also found that viral RNA in the skin culture media increased for both infections (Figure 2). Furthermore, in cryo-sectioned skin, immunohistochemical detection of MAYV and ZIKV showed widespread infected cells after 4 days (Figure 3), consistent with viral RNA detection in the homogenized tissue (Figure 2). Therefore, cultured human skin was viable and susceptible to arbovirus infection for up to 4 days.

Human skin processed similarly and infected with dengue virus 2 showed the presence of negative-stranded RNA at 48 hours and 72 hours after infection, indicative of viral replication (Limon-Flores et al., 2005). ZIKV infects several skin cell populations. Infection in primary cultures of epidermal keratinocytes (KCs) and dermal fibroblasts show increasing viral RNA loads and infectious titer over time (Hamel et al., 2015). Dermal dendritic and Langerhans cells, present in the dermis and epidermis, respectively (Pasparakis et al., 2014), are also permissive to ZIKV infection when derived from PBMCs (Hamel et al., 2015). Our results showed increased replication of ZIKV in human skin explants over time, which parallel previous findings (Hamel et al., 2015), but also suggest that these viruses spread from the inoculation site and egress into the media. MAYV infection in human skin is not well characterized and to our knowledge previously reported, in this study, we first showed MAYV infection in human skin ex vivo. Alphaviruses such as Chikungunya virus also replicate in human skin cell populations (Matusali et al., 2019). Human skin fibroblasts, both primary and immortal, are susceptible to Chikungunya virus in vitro (Ekchariyawat et al., 2015; Sourisseau et al., 2007; Wichit et al., 2017). Chikungunya virus-infected human skin explants showed the presence of viral RNA at 24 hours and 48 hours after infection when infected with a larger inoculum (10^5) (Bryden et al., 2020). Interestingly, both primary human and immortalized KCs poorly replicate Chikungunya virus by restricting

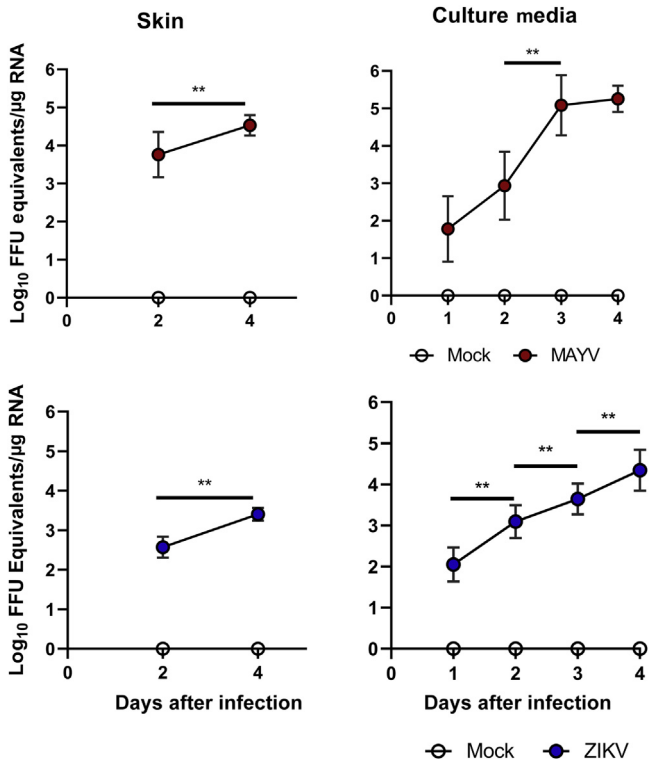

Figure 2. Skin is susceptible to arboviruses. Skin was infected intradermally with either MAYV (red) or ZIKV (blue). Data points are mean values with error bars indicating SDs. Data represents repeated independent experiments using n = 4 biological replicates per group across multiple donated tissues. A two-way ANOVA was used to determine statistical difference with Šidák's multiple comparisons. $^{**}P < 0.001$. FFU, focus forming units: MAYV, Mayaro virus; ZIKV, Zika virus.

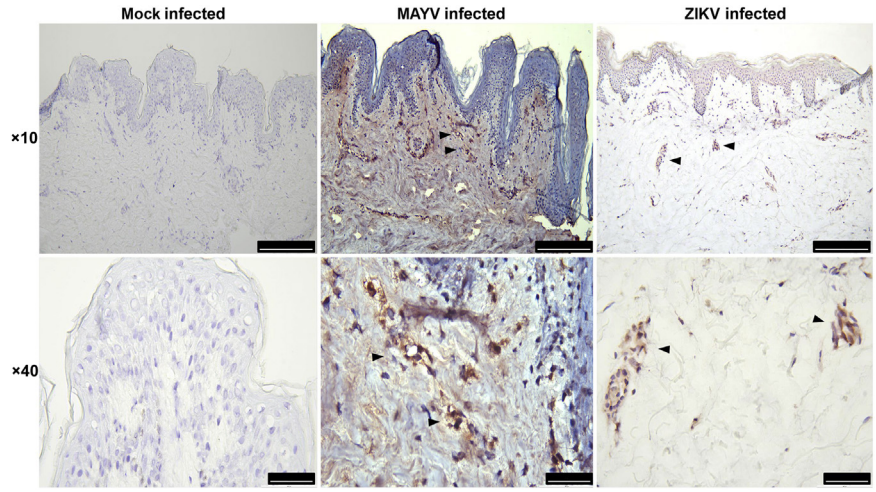

Figure 3. Expression of viral antigen in human skin. Immunohistochemical detection of MAYV antigen (middle column) and ZIKV antigen (right column) in cryo-sectioned skin after infection. Arrows indicate antigen detection at ×10 and ×40 magnification. Mock tissues were treated with either MAYV or ZIKV antibodies in parallel to respective infected tissues. Skin sections are representative of multiple biological replicates from independent experiments with consistent detection of viral antigen. Bar = 250 μm (×10 image) and 50 μm (×40 image). MAYV, Mayaro virus; ZIKV, Zika virus.

replication at a postendosomal fusion step, despite the high multiplicity of infection in vitro (multiplicity of infection = 50) (Bernard et al., 2015).

MAYV and ZIKV induce inflammatory expression in the skin

Expression of proinflammatory signals from skin resident cell populations are critical for recruiting circulating myeloid cells to the site of infection (Pasparakis et al., 2014). Because this model uses skin detached from the microvasculature, one of the primary limitations is the influx of inflammatory cells to the site of infection. Therefore, we assessed the expression of inflammatory targets, which recruit myeloid cell populations to the site of infection. Chemoattractive chemokines CCL2, CCL3, CCL4, and CXCL8 were upregulated during MAYV and ZIKV infection (Figure 4). In other studies, dengue virus-infected KCs express CCL2, CCL3, CCL4, CCL5, and CXCL8 in a similar trend at 48 hours after infection (Duangkhae et al., 2018). The same dengue virus-infected culture also shows the expression of IL-1α, IL-1β, IL-10, and CCL20 at the same time point (Duangkhae et al., 2018). West Nile virus infection induces the expression of antiviral cytokines such as IFN-β, IL-28a, and IL-29 24 hours and 48 hours after infection in primary KCs (Garcia et al., 2018). In addition, expression of CXCL1, CXCL2, CXCL8, and CCL20 and cytokines IL-6 and TNF-α are also induced at the same time points (Garcia et al., 2018).

Elevated expression levels of non-TLR receptors of viral ligands, RIG-I, MDA5, and PKR were also found in ZIKV and MAYV infected tissues. RIG-I and MDA5 are cytosolic helicases that detect viral RNA and are critical for triggering innate immune responses to flaviviruses and alphaviruses (Akhrymuk et al., 2016; Chow et al., 2018; Kell and Gale, 2015). PKR is a pattern recognition receptor and an IFN-inducible gene product that triggers signaling cascades responsible for further IFN-1 activation and inhibition of viral protein synthesis, among other functions (Munir and Berg, 2013). Both MAYV and ZIKV infection induced an increase in the expression of RIG-I, MDA5, and PKR in these tissues (Figure 4). This corresponds to previous findings of synthetic dsRNA poly(I:C) initiating antiviral signaling in KCs (Kalali et al., 2008). The natural expression of proinflammatory and antiviral genes in skin explants provides a suitable model for studying the human skin's immediate immune signaling events.

IFN-induced transmembrane proteins (IFITMs) are strongly upregulated by IFN-1 and IFN-2 and localize to plasma and endocytic membranes to restrict virus entry (Bailey et al., 2014; Zhao et al., 2019). Given that IFITM molecules show restriction of ZIKV (Savidis et al., 2016) and MAYV (Franz et al., 2021) infection, we assessed the expression of IFITM1, IFITM2, and IFITM3 in human skin tissue infected with either ZIKV or MAYV (Figure 4). IFITM1 levels were elevated during ZIKV infection as expected; however, there was not a significant increase from 2 to 4 dpi. IFITM2 slightly increased above baseline at 4 days after infection, whereas IFITM3 remained near basal expression levels. MAYV infection induced a more robust IFITM expression. IFITM1 was elevated at 2 and 4 dpi, with statistically higher expression at 4 dpi. IFITM2 and IFITM3 were slightly elevated at 2 dpi but significantly increased at 4 dpi. Further experimentation would be necessary to better understand the role of these antiviral molecules in the skin in relation to virus infection at the mosquito bite site.

CONCLUSION

Skin is the largest organ of the human body that interfaces with external stimuli, including pathogens, and is permissive to arbovirus infection (Garcia et al., 2017). Blood-feeding mosquitoes deliver a virus from infected salivary glands along with a cocktail of pharmacologically active molecules. Several studies showed that mosquito-derived salivary factors induce greater morbidity and higher viremia when delivered with a pathogen in animal models (Pingen et al., 2016). This highlights the importance of understanding mosquito-specific factors that are active during transmission, and the need to characterize such molecules in human skin. Human skin can be used as an ex vivo experimental site of infection for alpha- and flaviviruses. Both MAYV and ZIKV replicate in human skin up to 4 days after infection and shed into the skin culture media. Infection in the skin leads to gene expression of chemotactic factors responsible for recruiting inflammatory cells, such as neutrophils and macrophages. In addition,

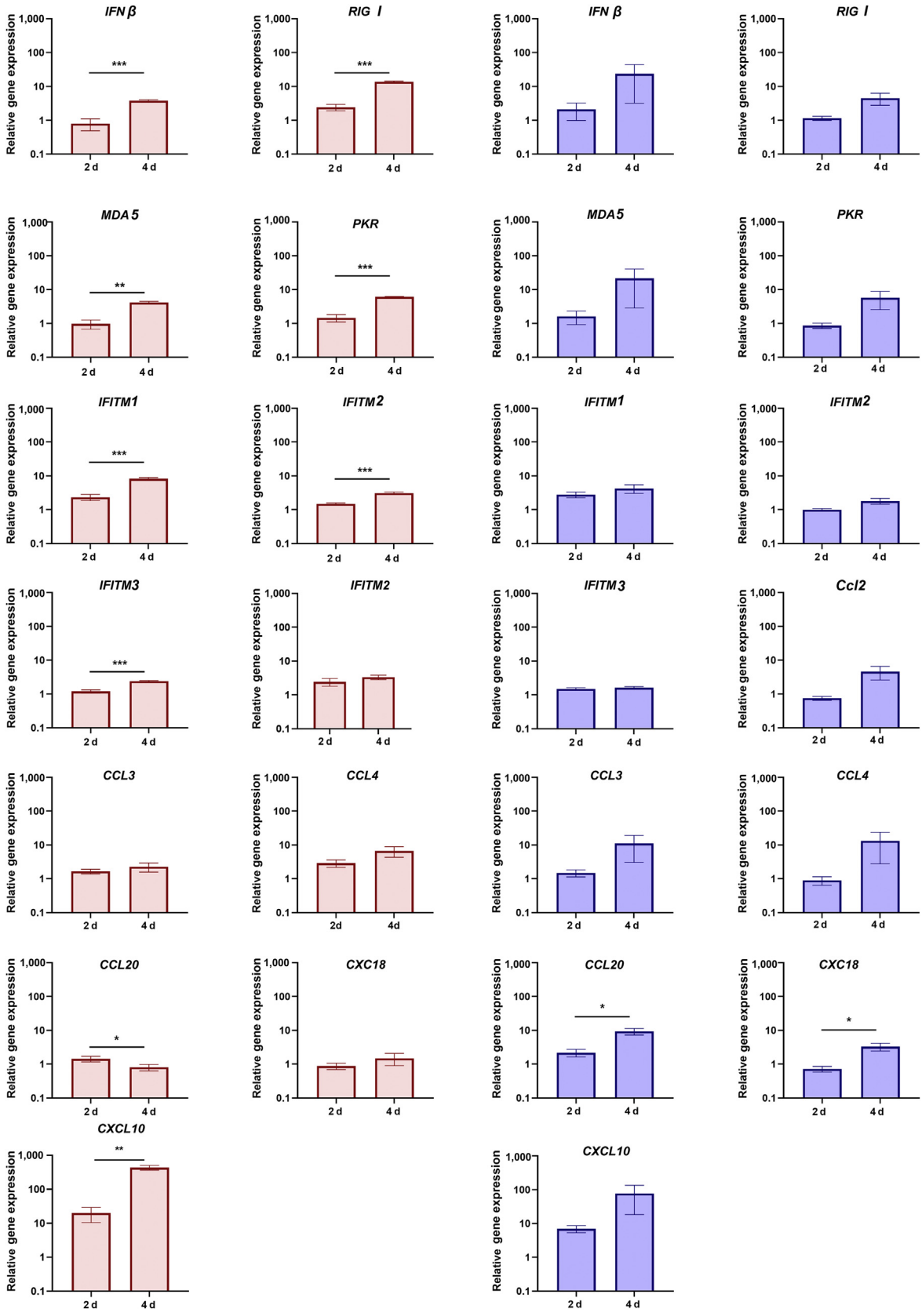

Figure 4. qPCR inflammatory gene expression of arbovirus infected human skin. qPCR analysis of MAYV infected tissues (red) and ZIKV infected tissues (blue) 2 and 4 d's after infection. Data shown is the relative fold change (Livak method $2^{-\Delta\Delta Ct}$) of virus-infected tissue compared with mock-infected tissue, normalized to 18S ribosomal RNA. Expression levels from 2 d to 4 d were compared for statistical difference. Error bars indicate the SEM. Data is representative of experimental means with SDs of independent experiments with repeat using n = 4 biological replicates per group. Student's *t*-test with Welch's correction was used to determine statistical difference. $^{*}P < 0.05$, $^{**}P < 0.001$, $^{***}P < 0.0001$. d, day; MAYV, Mayaro virus; ZIKV, Zika virus.

innate antiviral responses are active and induced after viral infection. Histological analysis showed no major pathological changes; however, immunohistochemical analysis showed widespread MAYV and ZIKV infection in human skin. Mosquito-borne virus replication in human skin can be used to further investigate mosquito transmission to humans and the associated salivary mediators that work in concert to facilitate blood acquisition and pathogen delivery.

MATERIALS AND METHODS

Ethics statement

All experiments involving deidentified human specimens were conducted in a biological safety level 2 laboratory in accordance with a protocol approved by the SUNY Upstate Medical University (Syracuse, NY) Institutional Review Board.

Culturing of cells and viruses

Vero, Vero E6, and C6/36 cells were obtained from ATCC (Manassas, VA) and were passaged in DMEM with 10% heat-inactivated fetal bovine serum and 1% penicillin-streptomycin at 37 °C + 5% carbon dioxide (Vero & Vero E6) or in Leibovitz L-15 media with 10% heat-inactivated fetal bovine serum, and 1% penicillin-streptomycin at 28 °C (C6/36) (Ammerman et al., 2008). ZIKV (Mex I44) was obtained from the World Reference Center for Emerging Viruses and Arboviruses at the University of Texas Medical Branch (Galveston, TX). MAYV (Uruma) was obtained from the Centers for Disease Control (Fort Collins, CO). Viruses were cultured in Vero cells (ATCC CCL-81) for four passages and then passaged once in C3/36 cells as referenced (Coelho et al., 2017; Moser et al., 2018). In addition, virus titers were obtained by focus-forming assay in Vero E6 cells as previously described (Rossi et al., 2012).

Preparation and infection of human skin

Deidentified adult human skin was donated by fully informed patients (written informed consent) undergoing reduction mammoplasty at the Upstate Medical University Hospital (Syracuse, NY). All skin specimens were collected within approximately 2 hours after surgery. Underlying adipose was grossly dissected, and each specimen was washed in PBS and incubated in skin culture media (RPMI 1640 media containing 10% heat-inactivated fetal bovine serum, 1% penicillin-streptomycin, and 0.25 μg/ml Amphotericin B) (Lloyd et al., 2020). The epidermis and upper dermal layers were removed using a skin grafting knife, cut into 1-cm^2 biological samples, then placed in Netwells (15 mm × 500 μm mesh size, Corning, Corning, NY) suspending the skin at a liquid-air interface. Netwells were placed in 12-well tissue culture plates containing 1 ml skin culture media. The skin was cultured ex vivo for 4 days in skin culture media at 33 °C with 5% carbon dioxide as previously described (Lloyd et al., 2020). Next, the skin was infected intradermally using a 28-gauge insulin syringe with 25 μl (±2 μL) of uninfected skin culture media (mock), ZIKV, or MAYV adjusted to deliver 10^3 focus forming units. Skin samples were processed as outlined below 2- and 4-days after infection. Each experimental group contained multiple biological replicates (n = 4) and independent infections were repeated using skin specimens from three donors.

RNA isolation, qRT-PCR, and gene expression analysis

On days 2 and 4 after infection, skin samples were cut in half using a scalpel and placed in either 10% neutral buffered formalin or OCT media for histological analysis or in TRIzol reagent for RNA isolation. RNA was extracted from the skin and skin culture media samples using TRIzol and TRIzol LS reagents, respectively, combined with Qiagen RNeasy mini kits (Qiagen, Hilden, Germany) to inactivate the virus and obtain high yields of RNA (Heinze et al., 2012; Hermance et al., 2020). RNA purity and concentration were verified on a DeNovix DS-11+ spectrophotometer (DeNovix, Wilmington, DE).

Absolute quantification of viral loads was performed using quantitative reverse transcriptase PCR (qRT-PCR), using a Bio-Rad CFX96 (Bio-Rad Laboratories, Hercules, CA). Viral genomes were amplified with the Bio-Rad One-Step Universal Probes kit using primers: ZIKV 1086, ZIKV 1162c, and probe ZIKV 1107-FAM or MAYV forward (5′- AAGCTCTTCCTCTGCATTGC-3′), MAYV reverse 2 (5′-TGCTGGAAATGCTCTTTGTA-3′), and MAYV probe (5′-GCCGAGAGCCCGTTTTTAAAATCAC-3′) previously established (Lanciotti et al., 2008; Waggoner et al., 2018). The MAYV primer-probe combination was slightly modified to use a Cy5/Iowa Black RQ fluorophore/quencher combination from Integrated DNA Technologies (Coralville, IA). RNA isolated from an aliquot of both ZIKV and MAYV, from the exact passage used for infection, was serially diluted and used to design a standard curve to quantify viral loads in tissue and supernatant.

Table 1. qPCR Primers Used for Gene Expression Analysis

Gene Target	Forward Primer (5′-3′)	Reverse Primer (5′-3′)	References
CCL2	GATCTCAGTGCAGAGGCTCG	TGCTTGTCCAGGTGGTCCAT	(Dumoulin et al., 2000)
CCL3	CATCACTTGCTGCTGACACG	TGTGGAATCTGCCGGGAG	(Duangkhae et al., 2018)
CCL4	ACCCTCCCACCGCCTGCTGC	GTTGCAGGTCATACACGTACT	(Dumoulin et al., 2000)
CCL5	ACCACACCCTGCTGCTTTGC	CCGAACCCATTTCTTTGC	(Dumoulin et al., 2000)
CCL20	TTGGATCCTGCTGCTACTCCACCTCTG	TTCTCGAGTATATTTCACCCAAGTCTGTTTT	(Akahoshi et al., 2003)
CXCL8	CTGGCCGTGGCTCTCTTGG	GGGTGGAAAGGTTTGGAGTATGTC	(Duangkhae et al., 2018)
CXCL10	GAAATTATTCCTGCAAGCCAATTT	TCACCCTTCTTTTTCATGTAGCA	(Clarke et al., 2010)
RIGI	AGTGAGCATGCACGAATGAA	GGGATCCCTGGAAACACTTT	(Surasombatpattana et al., 2011)
Mda5	TGTATTCATTATGCTACAGAACTG	ACTGAGACTGGTACTTTGGATTCT	(Surasombatpattana et al., 2011)
IFNβ	GACGCCGCATTGACCATCTA	TTGGCCTTCAGGTAATGCAGAA	(Surasombatpattana et al., 2011)
PKR	TCTGACTACCTGTCCTCTGGTTCTT	GCGAGTGTGCTGGTCACTAAAG	(Surasombatpattana et al., 2011)
IFITM1	GGGCATCCTCATGACCATTGGA	GGCTACTAGTAACCCCGTTTTTCCTG	(Prelli Bozzo et al., 2021)
IFITM2	GTCACCATGAACCACATTGTGCAAAC	CCCCCAGCATAGCCACTTCC	(Prelli Bozzo et al., 2021)
IFITM3	ACCATGAATCACACTGTCCAAACCTT	CCAGCACAGCCACCTCG	(Prelli Bozzo et al., 2021)
18S	GGCCCGAAGCGTTTACTTTG	GCCGGTCCAAGAATTTCACC	(Surasombatpattana et al., 2011)

cDNA conversion of tissue RNA was performed according to the manufacturer's specification using the Bio-Rad iScript cDNA synthesis kit using approximately 1 μg of RNA. cDNA was diluted five-fold, and gene expression analysis was performed using Bio-Rad iTaq Universal SYBR Green Supermix according to the manufacturer's specifications. Briefly, 1 μg of RNA/sample was used for the reverse transcriptase reaction. cDNA was diluted in RNase-free water at a 1:5 ratio, and a standard volume was used for each downstream qPCR reaction. Primers used for gene expression analysis are listed in Table 1. Expression was normalized using a eukaryotic ribosomal 18S as a housekeeping gene with data shown as a ratio of gene target fold change in infected tissue relative to mock-infected tissue using the Livak ($2^{-\Delta\Delta Cq}$) method (Livak and Schmittgen, 2001).

Histology and immunohistochemistry

Tissues fixed in formalin were paraffin-embedded and cut in 5 μm thick sections to be placed on glass slides (Hermance et al., 2016). Samples were deparaffinized and dehydrated in xylene and graded ethanol washes. H&E staining was performed according to the manufacturer's specifications (H-3502, Vector Laboratories, Burlingame, CA). Immunohistochemical detection of ZIKV and MAYV was performed using 5 μm frozen sections of tissues snap frozen in OCT media immediately after the indicated endpoint. Briefly, tissue sections were fixed in methanol then washed in Tris-buffered saline + 0.05% Tween 20. Wash buffer was applied between all blocking and antibody incubation steps. Sections were treated with BLOXALL solution (Vector Laboratories) to block endogenous peroxidases and alkaline phosphatases. Primary and secondary antibodies (murine immune ascites fluid generated against ZIKV or MAYV and goat anti-mouse horse-radish peroxidase conjugate, respectively) were incubated for 1 hour. Detection was performed with Vector Laboratories ImmPACT AMEC Red substrate, peroxidase kit. Cover slides were mounted using Vector Laboratories H5000 permanent mounting medium. Mock-infected tissues were sectioned and treated, in parallel, with the same antibody incubation and wash steps as listed above. All images were taken using a Leica DM2500 LED/DMC5400 brightfield microscope and Leica Application Suite X (LAS-X) software (Leica Microsystems, Wetzlar, Germany).

Data analysis

Statistical significance of viral growth kinetics was performed using two-way ANOVA with Šidák's multiple comparisons test in GraphPad Prism 9.1.2 (GraphPad Software, San Diego, CA). Statistical significance of gene expression data was analyzed by an F-test to determine variance, followed by a student's *t*-test to assess the increase of the target gene from 2 to 4 days after infection. Welch's correction was applied when the F-test hypothesis failed to be rejected.

Data availability statement

Data generated in the study are presented within this manuscript.

ORCIDs

Allen T. Esterly: http://orcid.org/0000-0003-1132-6797
Megan G. Lloyd: http://orcid.org/0000-0002-6034-0846
Prashant Upadhyaya: http://orcid.org/0000-0002-6992-1196
Jennifer F. Moffat: http://orcid.org/0000-0002-4371-8608
Saravanan Thangamani: http://orcid.org/0000-0002-4269-5993

AUTHOR CONTRIBUTIONS

Conceptualization: ST, ATE; Investigation: ATE, PU: ATE, JFM, MGL, ST; Funding Acquisition: ST; Data curation and Formal Analysis: ATE, ST; Resources: ST, PU, JFM; Supervision: ST; Writing - Original Draft Preparation: ATE; Writing - Review and Editing: ATE, JFM, MGL, PU, ST

CONFLICT OF INTEREST

The authors state no conflict of interest.

ACKNOWLEDGMENTS

The authors would like to acknowledge the anonymous donors for providing skin tissue used in this study. The study described in this manuscript was funded by Departmental Start-up funds and SUNY Empire Innovation Professorship funds to ST.

REFERENCES

Akahoshi T, Sasahara T, Namai R, Matsui T, Watabe H, Kitasato H, et al. Production of macrophage inflammatory protein 3alpha (MIP-3alpha) (CCL20) and MIP-3beta (CCL19) by human peripheral blood neutrophils in response to microbial pathogens. Infect Immun 2003;71:524–6.

Akhrymuk I, Frolov I, Frolova EI. Both RIG-I and MDA5 detect alphavirus replication in concentration-dependent mode. Virology 2016;487:230–41.

Ammerman NC, Beier-Sexton M, Azad AF. Growth and maintenance of Vero cell lines. Curr Protoc Microbiol 2008. Appendix 4:Appendix 4E.

Arcà B, Ribeiro JM. Saliva of hematophagous insects: a multifaceted toolkit. Curr Opin Insect Sci 2018;29:102–9.

Bailey CC, Zhong G, Huang IC, Farzan M. IFITM-family proteins: the cell's first line of antiviral defense. Annu Rev Virol 2014;1:261–83.

Bernard E, Hamel R, Neyret A, Ekchariyawat P, Molès JP, Simmons G, et al. Human keratinocytes restrict chikungunya virus replication at a post-fusion step. Virology 2015;476:1–10.

Bryden SR, Pingen M, Lefteri DA, Miltenburg J, Delang L, Jacobs S, et al. Pan-viral protection against arboviruses by activating skin macrophages at the inoculation site. Sci Transl Med 2020;12:eaax2421.

Castanha PMS, Erdos G, Watkins SC, Falo LD Jr, Marques ETA, Barratt-Boyes SM. Reciprocal immune enhancement of dengue and Zika virus infection in human skin. JCI Insight 2020;5:e133653.

Chow KT, Gale M Jr, Loo YM. RIG-I and other RNA sensors in antiviral immunity. Annu Rev Immunol 2018;36:667–94.

Clarke DL, Clifford RL, Jindarat S, Proud D, Pang L, Belvisi M, et al. TNFα and IFNγ synergistically enhance transcriptional activation of CXCL10 in human airway smooth muscle cells via STAT-1, NF-κB, and the transcriptional coactivator CREB-binding protein. J Biol Chem 2010;285:29101–10.

Coelho SVA, Neris RLS, Papa MP, Schnellrath LC, Meuren LM, Tschoeke DA, et al. Development of standard methods for Zika virus propagation, titration, and purification. J Virol Methods 2017;246:65–74.

Diagne CT, Bengue M, Choumet V, Hamel R, Pompon J, Missé D. Mayaro virus pathogenesis and transmission mechanisms. Pathogens 2020;9:738.

Duangkhae P, Erdos G, Ryman KD, Watkins SC, Falo LD Jr, Marques ETA Jr, et al. Interplay between keratinocytes and myeloid cells drives dengue virus spread in human skin. J Invest Dermatol 2018;138:618–26.

Dumoulin FL, Nischalke HD, Leifeld L, von dem Bussche A, Rockstroh JK, Sauerbruch T, et al. Semi-quantification of human C-C chemokine mRNAs with reverse transcription/real-time PCR using multi-specific standards. J Immunol Methods 2000;241:109–19.

Ekchariyawat P, Hamel R, Bernard E, Wichit S, Surasombatpattana P, Talignani L, et al. Inflammasome signaling pathways exert antiviral effect against chikungunya virus in human dermal fibroblasts. Infect Genet Evol 2015;32:401–8.

Franz S, Pott F, Zillinger T, Schüler C, Dapa S, Fischer C, et al. Human IFITM3 restricts chikungunya virus and Mayaro virus infection and is susceptible to virus-mediated counteraction. Life Sci Alliance 2021;4:e202000909.

Garcia M, Alout H, Diop F, Damour A, Bengue M, Weill M, et al. Innate immune response of primary human keratinocytes to West Nile virus infection and its modulation by mosquito saliva. Front Cell Infect Microbiol 2018;8:387.

Garcia M, Wehbe M, Lévêque N, Bodet C. Skin innate immune response to flaviviral infection. Eur Cytokine Netw 2017;28:41–51.

Hamel R, Dejarnac O, Wichit S, Ekchariyawat P, Neyret A, Luplertlop N, et al. Biology of Zika virus infection in human skin cells. J Virol 2015;89:8880–96.

Heinze DM, Wikel SK, Thangamani S, Alarcon-chaidez FJ. Transcriptional profiling of the murine cutaneous response during initial and subsequent infestations with Ixodes scapularis nymphs. Parasit Vectors 2012;5:26.

Hermance ME, Hart CE, Esterly AT, Reynolds ES, Bhaskar JR, Thangamani S. Development of a small animal model for deer tick virus pathogenesis mimicking human clinical outcome. PLoS Negl Trop Dis 2020;14:e0008359.

Hermance ME, Santos RI, Kelly BC, Valbuena G, Thangamani S. Immune cell targets of infection at the tick-skin interface during powassan virus transmission. PLoS One 2016;11:e0155889.

Huang YJS, Higgs S, Vanlandingham DL. Arbovirus-mosquito vector-host interactions and the impact on transmission and disease pathogenesis of arboviruses. Front Microbiol 2019;10:22.

Kalali BN, Köllisch G, Mages J, Müller T, Bauer S, Wagner H, et al. Double-stranded RNA induces an antiviral defense status in epidermal keratinocytes through TLR3-, PKR-, and MDA5/RIG-I-mediated differential signaling. J Immunol 2008;181:2694–704.

Kell AM, Gale M Jr. RIG-I in RNA virus recognition. Virology 2015. 479–80: 110–121.

Lanciotti RS, Kosoy OL, Laven JJ, Velez JO, Lambert AJ, Johnson AJ, et al. Genetic and serologic properties of Zika virus associated with an epidemic, Yap State, Micronesia, 2007. Emerg Infect Dis 2008;14:1232–9.

Limon-Flores AY, Perez-Tapia M, Estrada-Garcia I, Vaughan G, Escobar-Gutierrez A, Calderon-Amador J, et al. Dengue virus inoculation to human skin explants: an effective approach to assess in situ the early infection and the effects on cutaneous dendritic cells. Int J Exp Pathol 2005;86:323–34.

Livak KJ, Schmittgen TD. Analysis of relative gene expression data using real-time quantitative PCR and the 2 (-delta delta C(T)) method. Methods 2001;25:402–8.

Lloyd MG, Smith NA, Tighe M, Travis KL, Liu D, Upadhyaya PK, et al. A novel human skin tissue model to study varicella-zoster virus and human cytomegalovirus. J Virol 2020;94:e01082-20.

Maharaj PD, Widen SG, Huang J, Wood TG, Thangamani S. Discovery of mosquito saliva microRNAs during CHIKV infection. PLoS Negl Trop Dis 2015;9:e0003386.

Matusali G, Colavita F, Bordi L, Lalle E, Ippolito G, Capobianchi MR, et al. Tropism of the chikungunya virus. Viruses 2019;11:175.

Moser LA, Boylan BT, Moreira FR, Myers LJ, Svenson EL, Fedorova NB, et al. Growth and adaptation of Zika virus in mammalian and mosquito cells. PLoS Negl Trop Dis 2018;12:e0006880.

Munir M, Berg M. The multiple faces of proteinkinase R in antiviral defense. Virulence 2013;4:85–9.

Pasparakis M, Haase I, Nestle FO. Mechanisms regulating skin immunity and inflammation. Nat Rev Immunol 2014;14:289–301.

Pierson TC, Diamond MS. The continued threat of emerging flaviviruses. Nat Microbiol 2020;5:796–812.

Pingen M, Bryden SR, Pondeville E, Schnettler E, Kohl A, Merits A, et al. Host inflammatory response to mosquito bites enhances the severity of arbovirus infection. Immunity 2016;44:1455–69.

Pingen M, Schmid MA, Harris E, McKimmie CS. Mosquito biting modulates skin response to virus infection. Trends Parasitol 2017;33:645–57.

Prelli Bozzo C, Nchioua R, Volcic M, Koepke L, Krüger J, Schütz D, et al. IFITM proteins promote SARS-CoV-2 infection and are targets for virus inhibition in vitro. Nat Commun 2021;12:4584.

Rossi SL, Nasar F, Cardosa J, Mayer SV, Tesh RB, Hanley KA, et al. Genetic and phenotypic characterization of sylvatic dengue virus type 4 strains. Virology 2012;423:58–67.

Savidis G, Perreira JM, Portmann JM, Meraner P, Guo Z, Green S, et al. The IFITMs inhibit Zika virus replication. Cell Rep 2016;15:2323–30.

Sourisseau M, Schilte C, Casartelli N, Trouillet C, Guivel-Benhassine F, Rudnicka D, et al. Characterization of reemerging chikungunya virus. PLoS Pathog 2007;3:e89.

Styer LM, Kent KA, Albright RG, Bennett CJ, Kramer LD, Bernard KA. Mosquitoes inoculate high doses of West Nile virus as they probe and feed on live hosts. PLoS Pathog 2007;3:1262–70.

Surasombatpattana P, Hamel R, Patramool S, Luplertlop N, Thomas F, Desprès P, et al. Dengue virus replication in infected human keratinocytes leads to activation of antiviral innate immune responses. Infect Genet Evol 2011;11:1664–73.

Waggoner JJ, Rojas A, Mohamed-Hadley A, de Guillén YA, Pinsky BA. Real-time RT-PCR for Mayaro virus detection in plasma and urine. J Clin Virol 2018;98:1–4.

Weaver SC, Costa F, Garcia-Blanco MA, Ko AI, Ribeiro GS, Saade G, et al. Zika virus: history, emergence, biology, and prospects for control. Antiviral Res 2016;130:69–80.

Wichit S, Diop F, Hamel R, Talignani L, Ferraris P, Cornelie S, et al. Aedes aegypti saliva enhances chikungunya virus replication in human skin fibroblasts via inhibition of the type I interferon signaling pathway. Infect Genet Evol 2017;55:68–70.

Zhao X, Li J, Winkler CA, An P, Guo JT. IFITM genes, variants, and their roles in the control and pathogenesis of viral infections. Front Microbiol 2019;9:3228.